Supplementary Information

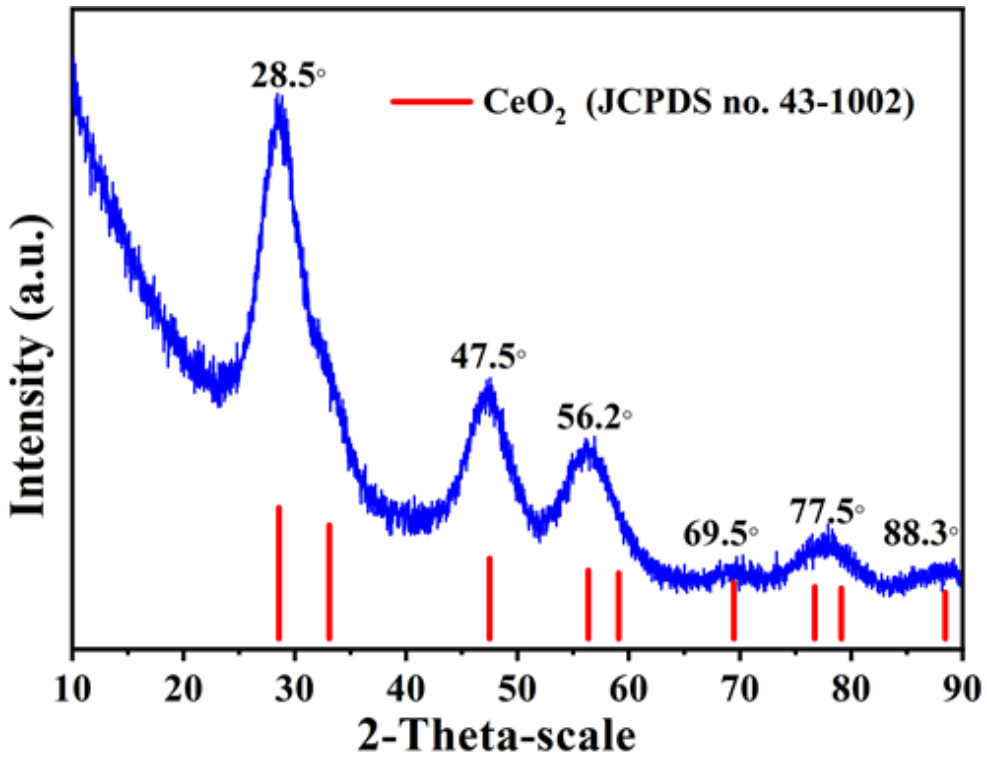


Fig. S1. XRD pattern of CMBO.

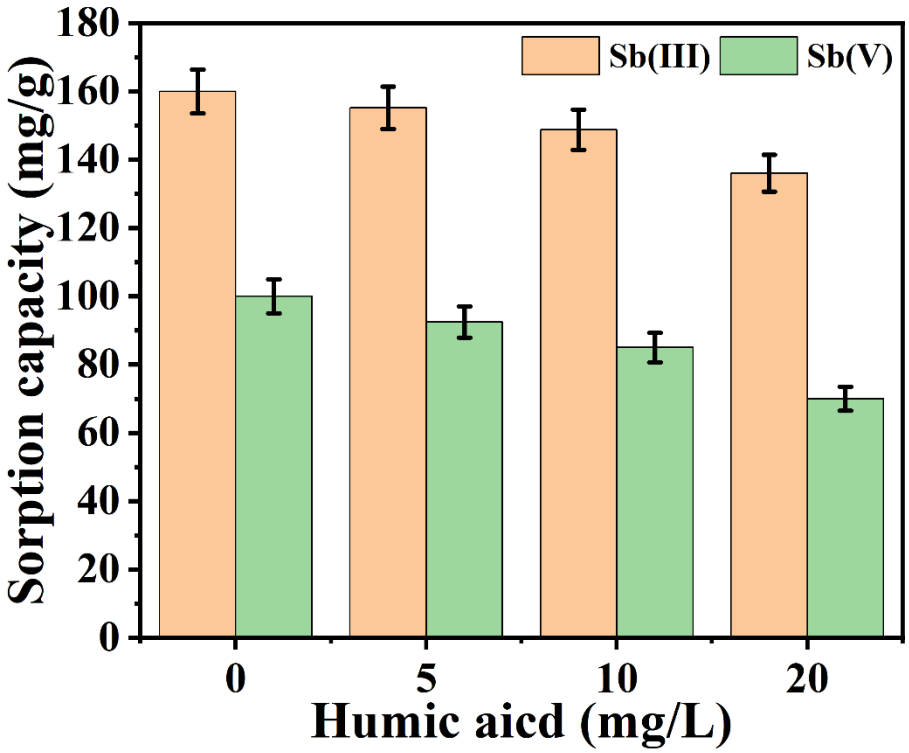


Fig. S2. Effect of humic acid on antimony sorption by CMBO.

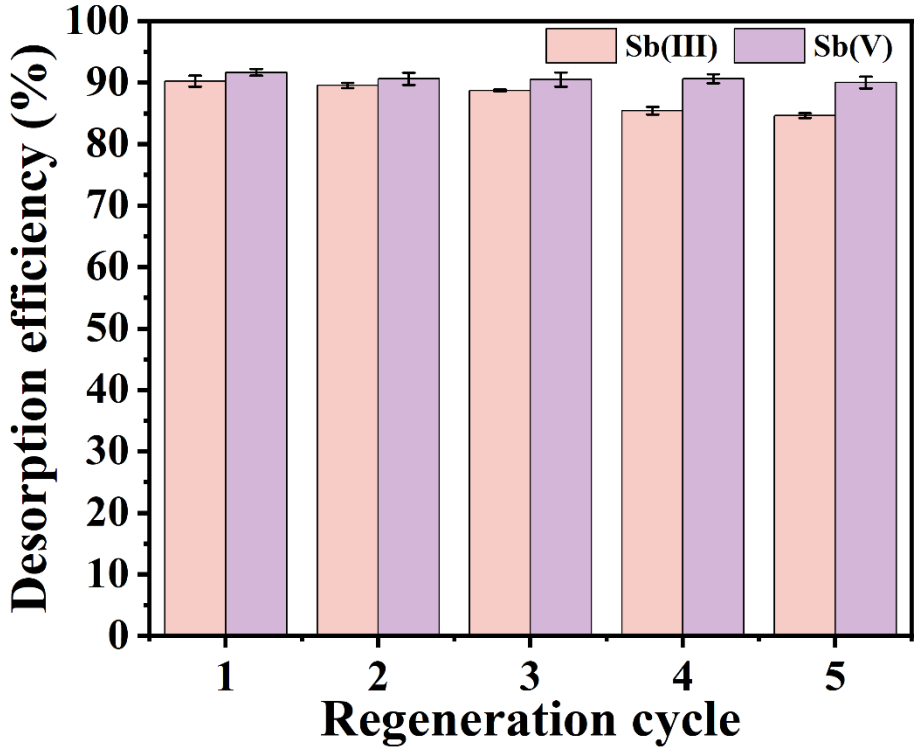


Fig. S3. Desorption efficiency of Sb(III) and Sb(V) from CMBO using 0.5 mol/L NaOH.

Table S1 Characteristics of the mine wastewater.

Water Samples	Items	Concentrations (mg/L)
Mining wastewater, Guizhou Province, China [a]	SO_4^{2-}	10846
	NO_3^-	5.0
	K	3.8
	Ca	433.5
	Na	74.5
	Mg	465.7
	Mn	250.2
	Fe	51.9
	Al	25.6
	Ni	1.4
	Sb	0.03

[a] The sampling point was situated at a mine outfall, located at a depth of 300 meters within the coal mine. The wastewater was mainly a mixture of groundwater and industrial wastewater generated during the mining process.

Table S2 Comparison of maximum antimony sorption capacities among different sorbents.

Item	Sorbents	Initial con. (mg/L)	Antimony state	Dosage (g/L)	Q_{max} (mg/g)	pH	Ref.
a	NaY@Ce	5~100	III V	1.0	24.7 7.3	7.0± 0.2	(Yan et al., 2020)
b	Ce-doped$_{(0.5)}$ Fe_3O_4	10~100	III V	0.2	224.2 188.1	7.0± 0.2	(Qi et al., 2017)
c	Ce/FeCP-BC	10~100	V	1.0	25.0	7.5	(Wang et al., 2019b)
d	$FMBO_3$	0.1~150	V	0.1	250.3	7.0± 0.1	(Yang et al., 2018)
e	FMBO	12~122	V	0.4	133.9	5.0	(Liu et al., 2015)
f	Mn-coated biochar	2~50	III V	50.0	0.9 0.7	2.0	(Jia et al., 2020)
g	MO-L-BC	1~60	III	0.2	248	5.0± 0.2	(Wan et al., 2020)
h	RGO/Mn_3O_4	10~1000	III V	1.0	151.8 105.5	6.8± 0.2	(Zou et al., 2016)
i	MO-2	10~500	III V	0.5	111.7 89.9	6.0	(Luo et al., 2017)
j	Co_3O_4@rGO	10~300	III V	1.0	151.1 152.6	7.0± 0.2	(Jiang et al., 2020)
k	Zr-MOFs	2~500	III V	0.8	136.9 287.9	7.0	(Li et al., 2017)
l	Fe-Cu-Al oxide	5~60	V	0.2	169.1	7.0	(Wang et al., 2019a)
m	CMBO	5~80 5~50	III V	0.2	260.6 101.1	7.0± 0.1	**This study**

Table S3 Summary of the XPS spectra of CMBO before and after Sb(III) and Sb(V) sorption.

Element Content		Before Sorption (%)	CMBO@Sb(III) (%)	CMBO@Sb(V) (%)
Mn	Mn^{2+}	21.1	17.0 ↓	20.1 ↓
	Mn^{3+}	35.0	40.7 ↑	34.9 -
	Mn^{4+}	43.9	22.3 ↓	45.0 ↑
Ce	Ce^{4+}	80.8	71.9 ↓	81.1 -
	Ce^{3+}	19.2	28.1 ↑	18.9 -
O	M-O	53.0	57.1 ↑	55.1 ↑
	M-OH	34.8	29.1 ↓	30.7 ↓
	H_2O	12.2	13.8 ↑	12.2 -
Sb	Sb(III)	0	44.4	0
	Sb(V)	0	55.6	100

Note: The Mn^{4+} loss (21.6%) exceeds the Mn^{2+} gain (15.9%) because 5.7% of Mn^{4+} is arrested at the Mn^{3+} intermediate stage. This asymmetry is characteristic of stepwise 1-electron transfer ($Mn^{4+} \rightarrow Mn^{3+} \rightarrow Mn^{2+}$), not disproportionation.

Supplementary References

Jia X, Zhou J, Liu J, Liu P, Yu L, Wen B, Feng Y (2020). The antimony sorption and transport mechanisms in removal experiment by Mn-coated biochar. Science of the Total Environment, 724: 138158

Jiang H, Tian L, Chen P, Bai Y, Li X, Shu H, Luo X (2020). Efficient antimony removal by self-assembled core-shell nanocomposite of Co_3O_4@rGO and the analysis of its adsorption mechanism. Environmental Research, 187: 109657

Li J, Li X, Hayat T, Alsaedi A, Chen C (2017). Screening of Zirconium-Based Metal-Organic Frameworks for Efficient Simultaneous Removal of Antimonite (Sb(III)) and Antimonate (Sb(V)) from Aqueous Solution. ACS Sustainable Chemistry & Engineering, 5(12): 11496-11503

Liu R, Xu W, He Z, Lan H, Liu H, Qu J, Prasai T (2015). Adsorption of antimony(V) onto Mn(II)-enriched surfaces of manganese-oxide and FeMn binary oxide. Chemosphere, 138: 616-624

Luo J, Hu C, Meng X, Crittenden J, Qu J, Peng P (2017). Antimony Removal from Aqueous Solution Using Novel α-MnO_2 Nanofibers: Equilibrium, Kinetic, and Density Functional Theory Studies. ACS Sustainable Chemistry & Engineering, 5(3): 2255-2264

Qi Z, Joshi T P, Liu R, Liu H, Qu J (2017). Synthesis of Ce(III)-doped Fe_3O_4 magnetic particles for efficient removal of antimony from aqueous solution. Journal of Hazardous Materials, 329: 193-204

Wan S, Qiu L, Li Y, Sun J, Gao B, He F, Wan W (2020). Accelerated antimony and copper removal by manganese oxide embedded in biochar with enlarged pore structure. Chemical Engineering Journal, 402: 126021

Wang J, Chen J, Li Q, Zhang G (2019a). Novel nanostructured Fe-Cu-Al trimetal oxide for enhanced antimony(V) removal: synthesis, characterization and performance. Water Sci Technol, 79(10): 1995-2004

Wang L, Wang J, Wang Z, Feng J, Li S, Yan W (2019b). Synthesis of Ce-doped magnetic biochar for effective Sb(V) removal: Performance and mechanism.

Powder Technology, 345: 501-508

Yan R, Qiu Z, Bian X, Yang J, Lyu S, Zhou A (2020). Effective adsorption of antimony from aqueous solution by cerium hydroxide loaded on Y-tape molecular sieve adsorbent: Performance and mechanism. Colloids and Surfaces A: Physicochemical and Engineering Aspects, 604: 125317

Yang K, Zhou J, Lou Z, Zhou X, Liu Y, Li Y, Ali Baig S, Xu X (2018). Removal of Sb(V) from aqueous solutions using Fe-Mn binary oxides: The influence of iron oxide forms and the role of manganese oxides. Chemical Engineering Journal, 354: 577-588

Zou J-P, Liu H-L, Luo J, Xing Q-J, Du H-M, Jiang X-H, Luo X-B, Luo S-L, Suib S L (2016). Three-Dimensional Reduced Graphene Oxide Coupled with Mn_3O_4 for Highly Efficient Removal of Sb(III) and Sb(V) from Water. ACS Applied Materials & Interfaces, 8(28): 18140-18149